Extremely low frequency plasma turbulence recorded by the DEMETER satellite in the ionosphere over the Abruzzi region prior to the April 6, 2009, L'Aquila earthquake

Jan Błęcki[1,*], Małgorzata Kościesza[1], Michel Parrot[2], Sergey Savin[3], Roman Wronowski[1]

[1] Space Research Centre PAS, Warsaw, Poland

[2] Laboratoire de Physique et Chimie de l'Environnement et de l'Espace, Université d'Orléans, CNRS, Orléans, France

[3] Space Research Institute, Russian Academy of Sciences, Moscow, Russia

ABSTRACT

The present study analyzes the low frequency fluctuations of the magnetic and electric fields prior to the earthquake with magnitude M ≈ 6.3 on April 6, 2009, in the Abruzzi region in Italy. This includes the disturbances of the ionospheric electromagnetic field prior to the earthquake, starting two weeks before the event, with detailed analysis for the days of March 26, April 1, April 2, and April 4, as 11, 5, 4 and 2 days prior to the earthquake, when the effects observed were strongest. Special attention is given to the characteristics of the spectra of these variations and the search for nonlinear effects. This analysis is possible in the time intervals when the extremely low frequency waveform was transmitted. Although the mechanism of the energy transmission from the earthquake preparation zone to the ionosphere is not determined, it can be said that the ionospheric plasma is an unstable medium and that even a small perturbation can lead to variations in the electromagnetic field and plasma parameters. Some aspects of this are discussed in the present report. The observations by the DEMETER satellite that are discussed suggest the presence of plasma turbulence over an area above the Abruzzi earthquake that occurred on April 6, 2009. The characteristics of the observed disturbances are studied through wavelet and bispectral analysis, the tools that are most relevant to the analysis of plasma turbulence. Furthermore, some statistical features are also presented, including the probability distribution function, and the kurtosis and skewness recently introduced into studies of such turbulence.

1. Introduction

The electromagnetic effects associated with earthquakes have been discussed for a long time. There are many reports and books that discuss this problem and have published observations that have originated from ground-based observatories and from satellites [Fraser-Smith et al. 1990, Hayakawa and Molchanov 2002, Parrot 1995, Parrot et al. 2006a, Pulinets and Boyarchuk 2004]. The DEMETER satellite provides the first possibility for a global study of the electromagnetic pre-seismic emissions using a set of experiments that lead to a more complete view of such phenomena.

Some results of the observations of the extremely low frequency (ELF) turbulence over seismically active regions by the DEMETER satellite have already been reported [Błęcki et al. 2009, 2010, 2011]. Here, we present an analysis of the electric field disturbances in the ELF range registered by DEMETER over the Abruzzi region prior to the April 6, 2009, L'Aquila earthquake. We discuss the response of the ionospheric plasma for the disturbance that originated with high probability from the lithosphere. The case of this April 6, 2009, earthquake in Abruzzi is an excellent example for this kind of study. The DEMETER satellite flew close to the epicenter of the earthquake many times when in burst mode (high bit-rate data acquisition), and the geomagnetic conditions were very quiet during a two-week period prior to the earthquake ($K_p < 3$). There were also no external sources of disturbances. Under these circumstances, we can study the ionospheric disturbances over the seismic area and assume with high probability that the perturbations are generated by some factors that have their source at the hypocenter of the earthquake. The possible mechanism of the energy transport from the ground to the ionosphere, and the source of these disturbances, are not discussed in this report. The mechanism that could perturb the ionosphere during the preparation for an earthquake are related to the redistribution of charges at the Earth surface, the emission of radioactive gas (radon), and/or the propagation of acoustic gravity waves. These mechanisms have been studied previously in the literature [see for example, Pulinets and Boyarchuk 2004, and references therein]. The ionospheric plasma can be very easily disturbed, and these disturbances can reach the nonlinear stage that can lead to the development of turbulence. In the ionosphere and

under magnetically quiet conditions, this turbulence is generally not observed at mid-latitudes [Li 2007].

The coverage of the data gathered in the burst mode for this event were good. The waveform registered in this mode of operation allows wavelet, bispectral and statistical analysis to be performed, which are relevant to a study of the properties of the observed disturbances of the ionospheric plasma (see Section 3) over the Abruzzi region.

We discuss the turbulence over this seismic event. But what is this turbulence? This question has no clear answer. The definition of the turbulence in fluids, gases and plasma is still under discussion, although some essential features can be noted: many degrees of freedom (different scales), all of which are in nonlinear interactions (cross-scale couplings), which creates a cascade of energy from larger (lower frequencies) to smaller (higher frequencies) sizes. The main characterizations of turbulence are related to the shape of the power spectrum and the high-order spectral analysis [McComb 1990, Frisch 1995, Biskamp 2003, Zimbardo et al. 2010]. Recently, some characterization using statistical descriptions has provided a new approach to this problem. The probability distribution function (PDF) of the measured parameters (in our discussion, the intensity of the electric field) and its parameters, such as kurtosis and skewness, give the new parameterization of the turbulent process [see, for example, Verma 2004].

The theory of turbulence predicts a different slope of the spectra for the different types of turbulence:
Noncompressible turbulence (K-1941) $\Rightarrow$
$\Rightarrow k^{-5/3}$ Kolmogorow
　　　　Noncompressible isotropic MHD (IK-1965) $\Rightarrow$
$\Rightarrow k^{-3/2}$ Iroshnikov-Kraichnan
Noncompressible anisotropic MHD (SG-2000)$\Rightarrow$
$\Rightarrow k_{\perp}^{-2}$ Sridhar and Goldreich
Whistler turbulence (DB-1997) $\Rightarrow k^{-7/3}$.

For the discussed measurements, this parameter is given. Section 2 briefly describes the wave experiment that is part of the scientific payload of DEMETER. The methods of the analysis of the wave form to study the specific character of the electromagnetic emissions registered in the vicinity of the epicenter of this Abruzzi earthquake are described in Section 3. Section 4 is devoted to the presentation and interpretation of these data from this event, and our conclusions are presented in Section 5.

2. The experiment

DEMETER is a low-altitude satellite (710 km) that was launched in June 2004 into a polar and circular orbit, to measure electromagnetic waves all around the Earth, except in the auroral zones. In December 2005, the altitude of the satellite was decreased to 660 km. The ELF/VLF (Extremely Low Frequency/Very Low Frequency) range for the electric field is from constant field up to 20 kHz (ELF up to 1.25 kHz). There are two scientific modes: a survey mode where

the spectra of one electric and one magnetic component are computed onboard up to 20 kHz, and a burst mode where in addition to the onboard computed spectra, the waveforms of one electric and one magnetic field component are recorded up to 20 kHz. The choice of the component is carried out by telecomand sent from flight control center. The burst mode allows the performing of spectral analyses with higher time and frequency resolution. Details of the wave experiment can be found in Parrot et al. [2006b], Berthelier et al. [2006] and Cussac et al. [2006]. During the burst mode, the waveforms of the six components of the electromagnetic field are also recorded up to 1.25 kHz. This allows the performing of wave propagation analysis [Santolík et al. 2003].

3. Methods of analysis

3.1. Wavelet analysis

Traditional Fourier analysis is not relevant for the study of turbulence. The Fourier transform spreads information about the localized features over all of the scales, making it impossible to study the evolution of different scale structures simultaneously. The important property of wavelet transform is that the square of the wavelet coefficients can be interpreted as local energy and their statistics are easy to visualize and understand.

The usefulness of wavelet analysis in the study of turbulence was underlined by Farge [1992] in the context of coherent structures. The main advantage of using wavelet transform is that it preserves the information about the local features (e.g. singularities) of the signal, and allows reconstruction of the signal over a given range of scales. This property is of particular importance in the study of turbulence, which often shows coherent structures that are apparently related to nonlinear processes. Extensive discussion of wavelet transform and its applications to turbulence can be found in a number of books and review articles [Farge et al. 1996, Mallat 1998]. Applications of wavelet analysis to study turbulence in space plasma were discussed by Wernik [2002, 2005]. Furthermore, we use the complex Morlet wavelet, which is represented by the function of time t and central frequency w0. A more detailed description of these methods of analysis can be found in Błęcki et al. [2007, 2009]. The definitions of the calculated functions and the software description is contained in the manual of the SWAN package [Lagoutte et al. 1999].

3.2. Bispectral analysis

When we discuss the development of plasma turbulence and the cascade of the energy in the spectrum, the first step in this cascade and the fundamental process that is involved is the 3-wave interaction.

The resonance conditions for these processes are: $\omega_1 + \omega_2 = \omega_3$, $k_1 + k_2 = k_3$, where ω_1, ω_2 and ω_3 are the wave

frequencies, and k_1, k_2 and k_3 are the wave vectors of the interacting waves. Verification of these conditions is possible using the so-called bispectral analysis. This method for the study of plasma processes was first proposed by Kim and Powers [1978]. It allows the nonlinearly interacting wave modes to be found by computing the bispectrum of the signal, which gives the information about the phase coherence of these waves. A quantitative measure of the phase coherency can be obtained using the bicoherence spectrum The computer procedures for the application of methods of wavelet and bispectral analysis have been developed in the SWAN package [Lagoutte et al. 1999]. We used these for the processing of the data selected for this study. The first use of bispectral analysis for space plasma was given in Tanaka et al. [1987]. These methods of analysis were applied in our earlier study of nonlinear processes in the magnetospheric cusp [Błęcki et al. 2007].

3.3. Statistical description of the turbulence

Measuring the electric field intensity with high time resolution (2.5 kHz sampling frequency) allows the construction of the probability distribution function of the deviation of the electric field intensity from the mean value for the selected time interval. The character of this function indicates whether the phenomenon has random character with a PDF that is close to Gaussian, or it is intermittent and asymmetric, which is typical for turbulence. The useful parameters to study its character are skewness and kurtosis. The skewness is the third moment of the measured physical value, normalized by the variance:

$$S = \frac{\left\langle (x - X)^3 \right\rangle}{\left\langle (x - X)^2 \right\rangle^{3/2}}$$

where, x is the measured value (in our case, the electric field intensity), and X denotes its mean value.

A PDF that is symmetric about the mean will have zero skewness. All higher odd moments of such a symmetric PDF will also be identically zero. The skewness reveals information about the asymmetry of the PDF. Positive skewness indicates that the PDF has a longer tail for $x–X>0$ than for $x–X<0$. Hence, a positive skewness means that the variable x is more likely to take on large positive values than large negative values. The kurtosis (or flatness) is defined as the fourth momentum of the measured physical value normalized by the variance:

$$K = \frac{\left\langle (x - X)^4 \right\rangle}{\left\langle (x - X)^2 \right\rangle^2}$$

A PDF with longer tails will have a larger kurtosis than a PDF with narrower tails. A time series with most measurements clustered around the mean has low kurtosis, a time series dominated by intermittent extreme events has high kurtosis. The kurtosis is the measure of the intermittency.

4. Observations

The earthquake discussed took place on April 6, 2009, at 01:32:41.4 UT in central Italy, in the Abruzzi region. It had a hypocenter located at 42.38°N and 13.32°E. Its depth was 2 km, and the magnitude was M≈6.3. The magnitude was not particularly strong, but the effects were unexpected: L'Aquila, the town closest to the epicenter, was in a great part destroyed.

The period of two weeks before the shock was geomagnetically very quiet (K_p index ≤3_). The data cover from the satellite DEMETER was very high, with full registration of the waveform of the electric and magnetic field variations in the ELF/VLF ranges. This gave the possibility to study the electromagnetic effects in the vicinity of the epicenter of this earthquake at a high scientific level, almost as in the laboratory.

An analysis of the ELF emissions in the vicinity of the epicenter was performed for the time period starting on March 26, so 11 days before the Abruzzi earthquake. An effect of increased intensity was registered even for this day, although the most intensive effects were seen on April 1 (5 days before the earthquake), April 2 (4 days before the earthquake) and April 4 (2 days before the earthquake). For these days, the electromagnetic emissions registered by DEMETER are presented in detail.

Figure 1 shows the orbit of the DEMETER satellite during the observations on April 1. The closest approach to the epicenter was at 20:37:00 UT, and the distance between the projection along the vertical line of the DEMETER position on the ground and the epicenter was 60 km. The wavelet spectrogram of the electric field in the ELF frequency
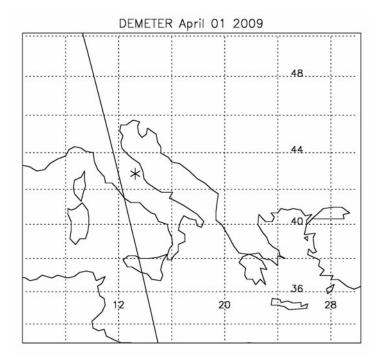

Figure 1. Map showing the epicenter of the April 6 L'Aquila earthquake (*) and the orbit of the DEMETER satellite on April 1, 2009. The point of closest approach is a larger distance from the epicenter (677 km).
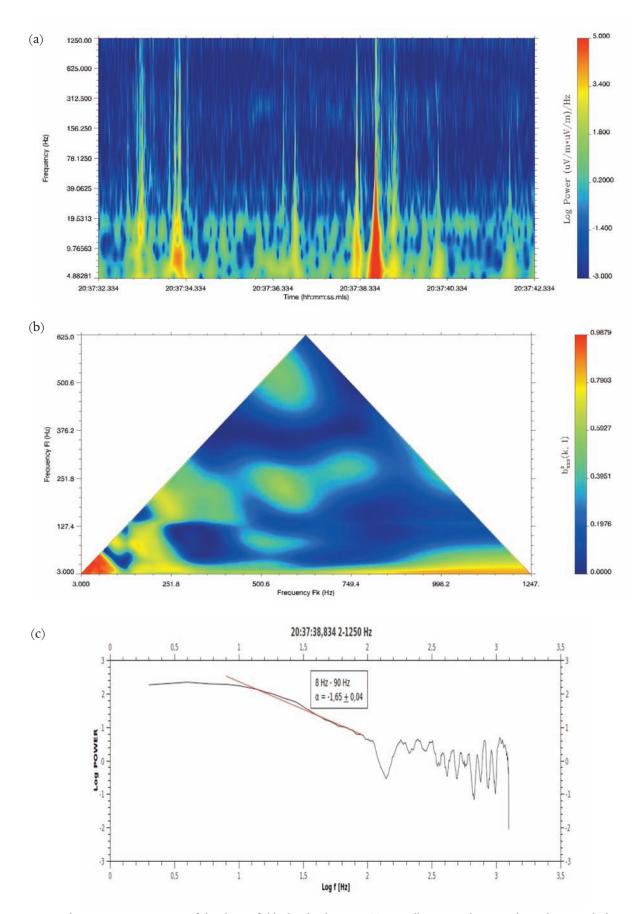
(a)

(b)

(c)

Figure 2. (a) Wavelet spectra up to 1250 Hz of the electric field taken by the DEMETER satellite on April 1, 2009, during burst mode, between 20:37:38 and 20:37:39 UT. The color scale represents the log of the power density of the electric field variations. (b) Bispectrum of the Ex signal in the ELF range. The horizontal and vertical axes of the frequencies of the waves are considered to find the interacting modes. The color scale represents the value of the bicoherence as a function of the frequencies. Two regions of strong 3-wave interactions can be seen: one in lower frequency range, and the other between 150 Hz and 400 Hz. (c) Single spectrum with slope $\alpha \approx -1.65$.
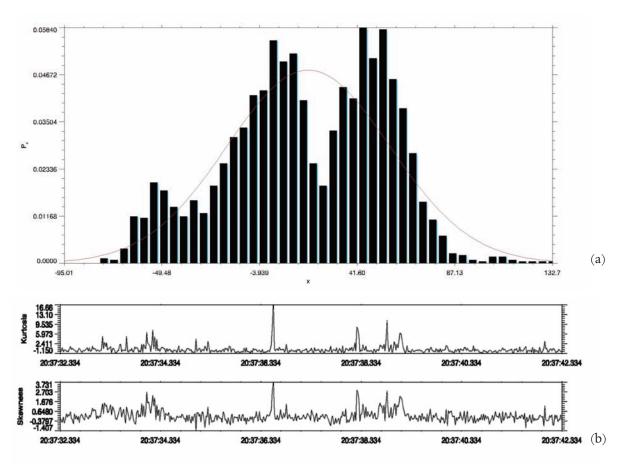
Figure 3. (a) Probability distribution function of the electric field intensity variations for the same time interval as in Figure 2. (b) Evolution of the kurtosis and skewness of the PDF between 20:37:32 and 20:37:42 UT.

range during a burst mode between 20:37:38 and 20:37:39 UT are presented in Figure 2a.

A strong enhancement of the wave activity and intensity of the waves is seen around the center of this time interval. The characteristic enhancement of the intensity began at low frequency and developed into the entire frequency range. The time resolution given by the wavelet analysis reveals the detailed structures of the spectrum and its evolution from lower frequency (5-10 Hz) to higher frequency around 20:37:38.535 UT, when DEMETER was very close to the epicenter. The strongest emissions are in a frequency range from a few tens of Hz up to 200 Hz, which is well below the proton gyrofrequency, the frequency with which the protons perform their rotation around the magnetic field line. This lower frequency band might correspond to the gyrofrequency of the oxygen ions O^+, which is of the order of 34 Hz.

The bispectrum for this disturbance is given in Figure 2b. This indicates a very strong significant 3-wave interaction that is clearly seen in the two frequency ranges: one in the lower frequency range, and another between 150 Hz and 400 Hz. Figure 2c shows the example of the single spectrum. The slope of this is about -1.623, which corresponds to the Kolmogorov model of the turbulence.

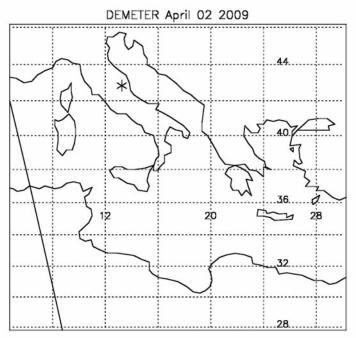Figure 3a shows the PDF, and the distortion of this plot can be seen in relation to a Gaussian distribution. The

Figure 4. Map showing the epicenter of the April 6 L'Aquila earthquake (*) and the orbit of the DEMETER satellite on April 2, 2009. The point of closest approach from the epicenter was 60 km.

parameters of the distribution, as kurtosis and skewness, are presented in Figure 3b. Strong enhancement of these moments were seen at the time of the wave activity increase.

This shows the intermittent character of the process, which is a sign of the turbulence.

The next day, similar strong emissions in the area of the Abruzzi earthquake were registered by the DEMETER satellite:April 2, 2009: 4 days before the event. The orbit of the DEMETER satellite during this observation on April 2 is given in Figure 4. The closest approach to the epicenter was at 21:05:30 UT and the distance between the projection
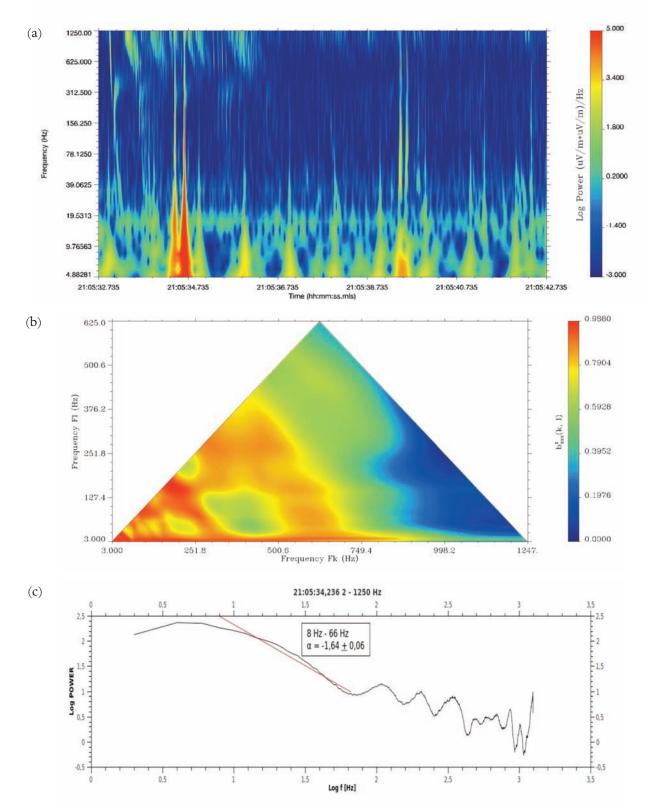

Figure 5. (a) Wavelet spectrogram of the broad-band emission in the ELF range at a greater distance from the epicenter (677 km), although still in the zone of seismic influence, in terms of a Dobrovolsky definition. The color scale is as in Figure 2. (b) Bispectrum of the Ex signal in ELF range. For description, see Figure 2b. The pattern of the frequency regions with strong 3-wave interactions is more complicated than for April 1, although a clear signature of the turbulent cascade is seen in the lower part of the panel. (c) Single spectrum with slope $\alpha \approx -1.64$.

along the vertical line of the DEMETER position on the ground and the epicenter was much greater, at 677 km. However, the most interesting recordings were obtained at 21:05:34 UT. Figure 5a shows the wavelet spectrogram of the electric field in the ELF frequency range during a burst mode between 21:05:34 and 21:05:35 UT. Figure 5b shows the bispectrum of the Ex signal in the ELF range. The pattern of the fr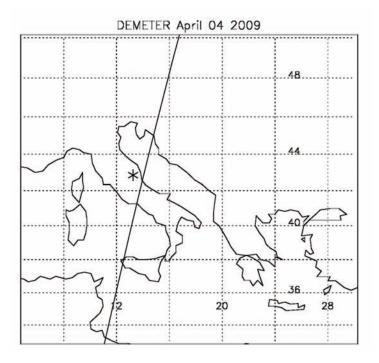equency regions with strong 3-wave interactions is more complicated than for April 1, but a clear picture of the turbulent cascade is seen in the lower part of Figure 5b. The cascade of the energy appears in the Figure 5b as an elongated 'red island' parallel to the horizontal frequency axis, from a few tens of Hz up to 250 Hz, the frequency where the whistlers are particularly enhanced up to highest frequency. Figure 5b shows us that the energy from the lower frequency was transferred to the higher frequency during the development of the turbulence. Figure 5c contains a single spectrum, and again the slope $\alpha \approx -1.639$ indicates the developed Kolmogorov type of the turbulence

The strongest emissions are focused in a frequency range from a few Hz up to 350 Hz, which is well below the proton gyrofrequency. The wavelet analysis underlines a wave band with a strong intensity at around 40 Hz. This frequency band might correspond to the gyrofrequency of the oxygen ions O^+, which is of the order of 34 Hz.

The next day with intensive ELF emissions was April 4. The orbit of the DEMETER satellite is shown in Figure 6. The closest approach to the epicenter took place at 20:29:00 UT, and this was 125 km. However, the most interesting event appeared at 20:28:32 UT when the distance between projection of the DEMETER position onto the ground and the epicenter was 280 km.

Figure 7a shows the wavelet spectrogram for the time interval of 20:28:30 to 20:28:40 UT. The short duration of the enhancement is seen at 20:28:33 UT. The bispectrum calculated for a 1-s interval around this disturbance shows a strong interaction around the frequency of 200 Hz, and in band 500 Hz to 700 Hz in the lower part of the frequency band, and again the cascade from 100 Hz up to 1000 Hz
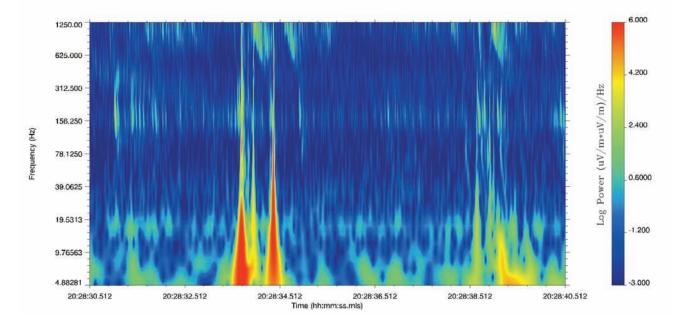

Figure 6. Map showing the epicenter of the April 6 L'Aquila earthquake (*) and the orbit of the DEMETER satellite on April 4, 2009. The point of closest approach from the epicenter was 125 km.

Figure 7a. Wavelet spectrogram of the broad-band emission in the ELF range recorded on April 4, 2009. The distance of the footprint of the satellite to the epicenter was about 280 km. The color scale is as in Figure 2.
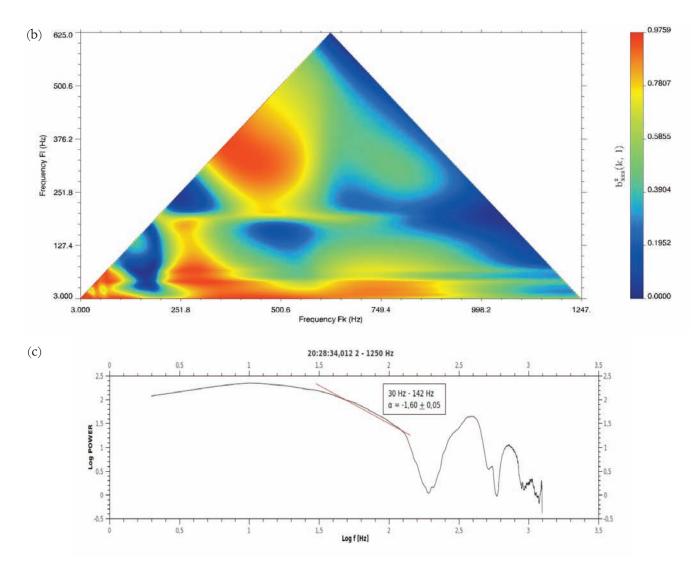
(b)

(c)

Figure 7b,c. (b) Bispectrum of the Ex signal in the ELF range. For description, see Figure 2b. The pattern of the frequency regions with strong 3-wave interactions is more complicated than for April 1. A clear picture of the turbulent cascade is seen in the lower part of the panel. (c) Single spectrum with slope $\alpha \approx -1.60$.

(Figure 7b). The single spectrum suggests the Kolmogorov type of the turbulence.

Figure 8 shows the data of the analysis of the ELF signal propagation during the time interval between 20:27:32 and 20:31:30 UT. The two upper panels in Figure 8 show the spectrum of the magnetic and electric field fluctuations. The next two panels in Figure 8 give the information on the polarization of the waves, which is in agreement with the polarization of the electron whistlers at higher frequencies. As usual at lower frequencies, the proton whistlers have a frequency band that is limited by the proton gyrofrequency (given by a model of the Earth magnetic field), and they have opposite polarization, as it is seen in Figure 8. Proton whistlers are usually generated by the same lightning strikes as the electron whistlers [Stefant 1985], although for this event, the most powerful electron whistlers are not associated with the most powerful proton whistlers, as can be seen in the next two panels of Figure 8. The changes in the atmospheric electric field during the

preparation phase of the earthquake can be a source of similar emissions. These panels in Figure 8 show the direction of propagation relative to the Earth magnetic field [Santolík and Parrot 1999]. The fifth panel in Figure 8 shows the angle between the magnetic field and the Poynting vector. It can be seen that this angle is close to the 180° for the proton whistlers, which means that the wave propagation is opposite to the magnetic field direction, and for the northern hemisphere, that the wave is coming from a region below the satellite. This information is confirmed in the bottom panel of Figure 8, where the z-component of the Poynting vector is shown. Its negative value also indicates that the origin of the proton whistlers is below the satellite orbit and that the origin of the electron whistlers is from the southern hemisphere. This confirms that the natural waves are coming from the ionosphere below the satellite, and are probably generated by the ionospheric effects that have a source in the processes associated with the preparation for the earthquake.
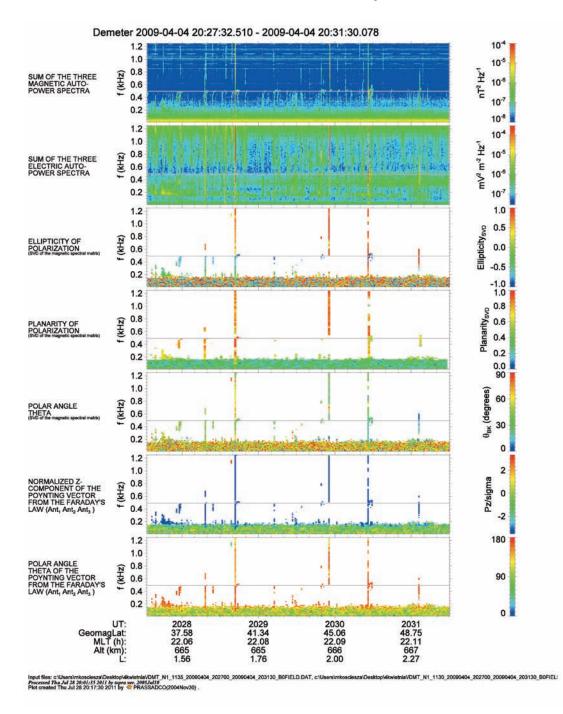
Figure 8. Detailed propagation analysis of a part of the ELF signal registered on April 4, 2009, as a function of time. Top to bottom: the two first panels show the spectrum of the magnetic and electric field variations (sum of the 3 components), the third panel shows the ellipticity of the magnetic field polarization. A value of 1 means right-hand circularly polarized waves; linear polarization gives 0; and −1 indicates left-hand circular polarization. The fourth panel is the sense of the polarisation of the waves, and the fifth panel indicates the angle between the Poynting vector and the Earth magnetic field, as calculated by the singular value decomposition technique [Santolík et al. 2003]. The bottom panel shows the z-component of the Poynting vector. Empty areas in the four bottom panels correspond to magnetic power-spectral densities below 10^{-7} nT² Hz^{-1}. In each panel, the black line is related to the proton gyrofrequency. The geomagnetic latitude and the magnetic local time (MLT) are displayed at the bottom of the figure according to the Universal Time (UT).

5. Conclusions

In the present study, the electromagnetic effects observed by the DEMETER satellite prior to the earthquake in central Italy have been presented and discussed. The analysis of the wave forms in ELF frequency range with the wavelet and bispectral methods shows strong emissions in this frequency range in the ionosphere 5, 4 and 2 days before the earthquake. The results discussed were obtained during a very quiet time, and therefore no ionospheric and magnetospheric sources of perturbation were expected. However, these turbulence behaviors are not specifically related to the occurrence of earthquakes, and can be seen in other regions of the ionosphere, particularly at equatorial and high latitudes [Molchanov 2004, Li 2007]. However, the

coincidence in space and time of the recorded disturbances with this earthquake suggests that the effects observed at the mid-latitudes are related to a perturbation of the ionosphere that might be associated with the preparation for this Abruzzi earthquake. The statistical behavior of the signal (intermittent) and the shape of the spectra, suggest that turbulence observed during this event is of the Kolmogorov type.

References

Berthelier, J.J., M. Godefroy, F. Leblanc, M. Malingre, M. Menvielle, D. Lagoutte, J.Y., Brochot, F. Colin, F. Elie, C. Legendre, P. Zamora, D. Benoist, Y. Chapuis, J. Artru and R. Pfaff (2006). ICE-the electric field experiment on DEMETER, Planet. Space Sci., 54, 456-471.

Biskamp D. (2003). Magnetohydrodynamic Turbulence, Cambridge University Press, Cambridge.

Błęcki, J., S. Savin, M. Parrot and R. Wronowski (2007). Nonlinear interactions of the low frequency plasma waves in the middle-altitude polar cusp as observed by Prognoz-8, Interball-1 and cluster satellites, Acta Geophys., 55, 459-468.

Błęcki, J. , M. Parrot and R. Wronowski (2009). Can the Ionospheric Plasma Turbulence be a Precursor of the Earthquake? Results of DEMETER Measurements, In: Proceedings of ESA Swarm Science Workshop, Potsdam 24-26 June.

Błęcki, J. , M. Parrot and R. Wronowski (2010). Studies of the electromagnetic field variations in ELF frequency range registered by Demeter over the Sichuan region prior to the 12 may 2008 earthquake, Int. J. Remote Sens.; doi: 10.1080/01431161003727754.

Błęcki, J., M. Parrot and R. Wronowski (2011). Plasma turbulence in the ionosphere prior to earthquakes, some remarks on the DEMETER registrations, J. Asian Earth Sci.; doi: 10.1016/j.jseaes.2010.05.016, 41, 450-458.

Cussac, T., P.M.A. Ultre-Guerard, F. Buisson, G. Lassalle-Balier, M. Ledu, C. Elisabelar, X. Passot and N. Rey (2006). The DEMETER microsatellite and ground segment, Planet. Space Sci., 54, 413-427.

Farge, M. (1992). Wavelet transforms and their applications to turbulence, Annu. Rev. Fluid Mech., 24, 395-457.

Farge, M., N. Kevlahan, V. Perrier, and É. Goirand (1996). Wavelets and turbulence, P. IEEE, 84, 639-669.

Fraser-Smith, A.C., A. Bernardy, P.R. McGill, M.E. Ladd, R.A. Helliwell and O.G. Jr. Villard (1990). Low frequency magnetic field measurements near the epicenter of the Ms 7.1 Loma Prieta earthquake, Geophys. Res. Lett., 17, 1465-1468.

Frisch, U. (1995). Turbulence. The legacy of A.N. Kolmogorov, Cambridge University Press, Cambridge.

Hayakawa, M. and O.A. Molchanov (2002). Seismo Electromagnetics: Lithosphere-Atmosphere-Ionosphere Coupling, Terra Scientific Publishing Company TERRAPUB, Tokyo.

Kim Y.C. and E.J. Powers (1978). Digital bispectral analysis of self-excited fluctuation spectra, Phys. Fluids, 21, 1452-1453.

Lagoutte, D., J.Y. Brochot and P. Latremoliere (1999). SWAN Software for Waveform Analysis, Analysis Tools version 2.3, LPCE/NI/003.D - Part 1, Part 2 Part 3.

Li, F. (2007). Etude dans l'ionosphère de la densité électronique et de la turbulence électrostatique en fonction de l'activité séismique, PhD thesis, University of Orléans, France.

Mallat, S. (1998). A Wavelet Tour of Signal Processing, Academic Press, San Diego.

McComb, W.D. (1990). The physics of fluid turbulence, Oxford Science Publications, Oxford.

Molchanov, O. A. (2004). On the origin of low- and middle latitude ionospheric turbulence, Phys. Chem. Earth, 29, 559-567.

Parrot, M. (1995). Electromagnetic noise due to earthquakes, In: Handbook of Atmospheric Electrodynamics, edited by H. Volland, CRC Press, Boca Raton, vol. II., pp. 95-116

Parrot, M., J.J. Berthelier, J.P. Lebreton, J.A. Sauvaud, O. Santolík and J. Błęcki (2006a). Examples of unusual ionospheric observations made by the DEMETER satellite over seismic regions, Phys. Chem. Earth, 31, 486-495.

Parrot, M., D. Benoist, J.J. Berthelier, J. Błęcki, Y. Chapuis, F. Colin, F. Elie, P. Fergeau, D. Lagoutte, F. Lefeuvre, C. Legendre, M. Leveque, J.L. Pincon, B. Poirier, H.C. Serana and P. Zamora (2006b). The magnetic field experiment IMSC and its data processing onboard DEMETER: scientific objectives, description and first results, Planet. Space Sci., 54, 441-455.

Pulinets, S.A. and K.A. Boyarchuk (2004). Ionospheric Precursors of Earthquakes, Springer, New York.

Santolík, O. and M. Parrot (1999). Case studies on wave propagation and polarization of ELF emissions observed by Freja around the local proton gyro-frequency, J. Geophys. Res., 104, 2459-2475.

Santolík, O., M. Parrot and F. Lefeuvre (2003). Singular value decomposition methods for wave propagation analysis, Radio Sci., 1010, 38; doi: 10.1029/2000RS002523.

Stefant, R.J. (1985). Comments on the proton whistler generation process, Planet. Space Sci., 33 (3), 333-349.

Tanaka, Y., D. Lagoutte, M. Hayakawa and F. Lefeuvre

(1987). Spectral broadening of VLF transmitter signals and sideband structure observed on Aureol-3 satellite at middle latitudes, J. Geophys. Res., 92, 7551-7559.

Verma, M.K. (2004). Statistical theory of magnetohydrodynamic turbulence, Phys. Rep., 401, 229-380.

Wernik, A.W. (2002). High-latitude ionospheric plasma turbulence: advanced analysis methods and results, Acta Geophys. Pol., 50, 119-134.

Wernik, A.W. (2005). Application of the wavelet transform to investigation of space plasma turbulence, In: Proceedings of the International Workshop on Applications of Wavelets to Real World Problems, edited by A. Hasan Siddiqi, S. Alsan, M. Rasulov, O. Oguz and Z. Aslan, Istanbul Commerce University Publication, Istanbul, 49-66 .

Zimbardo, G., A. Greco, L. Sorriso-Valvo, S. Perri, Z. Vörös, G. Aburjania, K. Chargazia and·O. Alexandrova, (2010). Magnetic turbulence in the geospace environment, Space Sci. Rev.; doi: 10.1007/s11214-010-9692-5.

---

*Corresponding author: Jan Błęcki,
Space Research Centre PAS, Warsaw, Poland;
email: jblecki@cbk.waw.pl.